Atomic Arrangements at Metal Surfaces

J. R. NOONAN AND H. L. DAVIS

The termination of a solid induces changes in the locations of the outermost atoms of the solid. The changes can be minor or as dramatic as the rearrangement of the atoms into a different crystallographic group. Surface crystallography studies have determined that all surfaces are altered by forces induced at the solid-vacuum interface. At the least, the outermost atomic layers are displaced away from positions that they would have had in the bulk environment. Results from experimental and theoretical investigations for the Al(110) surface are discussed to illustrate present understanding of the surface atomic displacements. Some effects that the truncation-induced forces have on the surfaces of binary metal alloys are also discussed.

THE TERMINATION OF A SOLID CREATES A SURFACE. THIS statement is so obvious that many of its consequences are often overlooked. For example, the corrosion and abrasion resistance of materials and the adhesion of adsorbate films depend more on surface properties than on bulk properties. The creation of a surface universally and fundamentally alters the atomic arrangement from the structure of the bulk. There are many examples of surfaces of semiconductor and metal crystals for which a different arrangement of atoms from the bulk has been demonstrated.

The differences are more easily understood for semiconductors than for metals. Because of the covalent bonding of semiconductors, bonds to an atom are broken when a surface is created. When the uncompleted bonds reform, the energy of reforming is usually enough to displace an atom from its bulk position. Therefore, the atomic arrangements of most semiconductor surfaces are altered from those of their bulk. The Si(111) surface is one intensely studied example of this phenomenon. When it is cleaned and well annealed, this surface is reconstructed—that is, its atoms are displaced from positions that they would occupy in a truncated bulk crystal—and the unit cell of the surface layer can be placed on a net of 49 silicon atoms that have the bulk atomic arrangement. The resulting low-energy electron diffraction (LEED) pattern is referred to as (7×7) because there are seven times more diffraction beams along each basis vector direction than there would be for the hypothetical truncated bulk. The complex "star" array of the LEED pattern is a good example of a surface being dramatically different from its bulk. Recent advances have been made in determining the atomic structure of the Si(111)-(7×7) surface (*1–3*).

The cohesion of metals is different from that of semiconductors. A metal can be represented, to first order, as a lattice of positive ions imbedded in a continuum density of conduction electrons. Thus the termination of a metal by a surface does not require that strong directional bonds be broken. The truncation of a metal, however, does alter the environment of the surface atoms. Although not as many metal surfaces exhibit reconstruction as semiconductors, there are several that do: the Au(100), (110), and (111) surfaces, the Pt(100) and (110) surfaces, the Ir(100) and (110) surfaces, the W(100) surface, and the Mo(100) surface. All of these have surface atomic arrangements different from their bulk arrangement, as revealed by their LEED patterns (*4*). These reconstructed surfaces illustrate that metal surface atoms are in a different environment than bulk atoms. Nevertheless, most metal surfaces exhibit the same two-dimensional atomic arrangement as the bulk; that is, the LEED pattern of most metal surfaces is the same as if the crystal were merely truncated. It should not be inferred, however, that these surfaces are merely the termination of bulk crystals. In fact, recent experimental and theoretical research has shown that such a simple model is incorrect. The response of surface atoms to electrostatic forces induced by the termination results in their displacement away from truncated bulk positions.

In 1972, two independent LEED studies reported that the outermost layer of atoms in the Al(110) surface was contracted toward the bulk such that the spacing between the surface atomic layer and the adjacent layer was reduced by about 10% with respect to the bulk spacing (*5, 6*). It is now understood that such relaxation of an atomic layer is a general phenomenon for metal surfaces. The termination of a metal causes the electronic charge at the surface to redistribute so that the electronic surface tension is reduced. Finnis and Heine (*7*) suggested that the new charge density then induces electrostatic forces on the atomic cores of the surface, and the surface layer atoms relax away from truncated bulk sites in such a way that the induced forces are canceled by the ion-ion interactions of deeper layers. It was realized subsequently that the electronic charge distribution could not recover in a single atomic layer. Therefore, the electron charge distribution and the atomic core positions change in not just one plane—the surface layer—but in deeper layers in the solid as well (*8*), yielding multilayer surface relaxation. The relaxation patterns, in which several outermost atomic layers are relaxed away from bulk positions, have been identified experimentally for a large number of metal surfaces (*9–11*).

Surface crystallographic studies have been extended to include binary metal alloys, and their results provide important information concerning atomic interactions at surfaces. Four effects have been found. The termination of a copper-aluminum alloy induces ordering of the aluminum atoms, which segregate to the surface even though they are randomly distributed in the bulk material (*12*). In the atomic layers at the (100) surface of the $Pt_{78}Ni_{22}$ alloy, the concentration of platinum is alternately enriched and depleted (*13*). The Ni_3Al(100) (*14*) and Cu_3Au(100) (*15*) surfaces have a preferential termination of their stacking sequences. The NiAl(110) surface is reconstructed such that the nickel atoms are displaced toward the bulk but the aluminum atoms are displaced away from the bulk (*16*). This information will be useful in theoretical modeling of atomic interactions at alloy surfaces. Such research has the potential to

---

J. R. Noonan and H. L. Davis are research scientists in the Solid State Division, Oak Ridge National Laboratory, P.O. Box X, Oak Ridge, TN 37831.

increase our understanding of even more complex problems in materials science. For example, as theories of the pair interactions at surfaces become more quantitative, they can be applied to the study of extended defects in solids, such as grain boundaries, epitaxial growth, and interfaces (which are examples of internal surfaces).

Modern Surface Crystallography

The quantitative analysis of surfaces has been driven by four principal developments: improvements in the accuracy of instrumentation, the development of new surface techniques, continuing improvements in theoretical formulations, and improvements in computers and numerical techniques. There are various techniques to study the crystallography of surfaces. Some of these techniques, such as LEED, ion backscattering, molecular scattering, x-ray scattering, and scanning tunneling microscopy, directly probe the atomic structure of the surface. Other methods, such as photoelectron and molecular vibrational spectroscopies, determine atomic structure indirectly; that is, measured features are compared with calculations for a given atomic arrangement. Although there are certain advantages for each of these techniques, LEED and ion backscattering have been particularly successful in analyzing the relaxations of metal surfaces, especially those with a surface symmetry identical to that of the bulk. This article describes experiments with LEED; the ion-scattering technique is discussed in an article by Tromp (*3*).

LEED is a remarkably durable surface technique. It was first used as a surface probe when Davisson and Germer (*17*) discovered electron diffraction from a nickel surface in 1926, and it is still one of the most precise surface techniques (*9–11*).

Surface crystallography is determined in LEED by measuring the elastically scattered electron current as a function of electron energy. Typically, LEED electrons have kinetic energies between 20 and 500 eV. There are two principal reasons why LEED is so sensitive to surface structure. First, electrons in the LEED energy range interact strongly with solids; therefore, the mean free path for the low-energy electrons is about 10 Å. Electrons that penetrate to any great depth in the solid cannot backscatter to the surface without losing energy; thus, the elastically backscattered electrons contain primarily surface information.

Second, electrons with energies of 20 to 500 eV have wavelengths that are comparable to the lattice spacings of atoms in the solid. For example, a 100-eV electron has a wavelength of 1.23 Å, and the spacing between adjacent aluminum atoms in a bulk crystal is 2.86 Å. In the case of single crystals, the electrons are coherently scattered by the solid into collimated beams. In other words, an ordered array of atoms in the surface acts as a two-dimensional grating, and the scattering electrons are focused into sharp diffraction beams that represent the two-dimensional reciprocal lattice of the surface's real-space lattice (Fig. 1). Furthermore, the modulation of the diffracted current as a function of energy is related to the coherent interference between the surface and deeper layers (*18*). There is no simple relation between peaks in the current and the surface's atomic structure, however.

Although the electrons are strongly attenuated, they also scatter from a large number of atoms before they exit the solid. Because of the strong multiple scattering of the low-energy electrons, the only way to determine the surface crystallography is to compare the experimental current-voltage relation, usually called the *I-V* spectrum, to *I-V* spectra calculated for various assumed structural models. The calculations also use nonstructural parameters to simulate the electron scattering, atomic vibrations, and beam attenuation. The procedure in a LEED analysis is then to test various structural models to find that model whose calculated *I-V* spectrum agrees best with the experimental spectra. The quality of the agreement between the calculated and measured *I-V* spectra has improved considerably over the past decade as a result of advances both in the theoretical formulation of LEED and in experimental measurements.

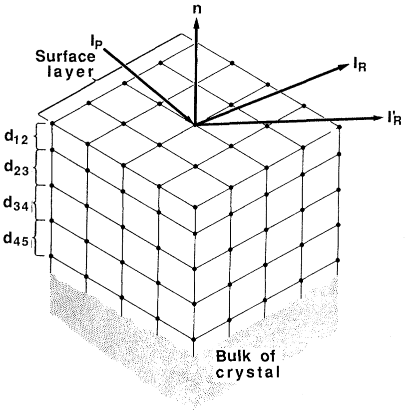

Fig. 1. Schematic representation of electron diffraction from a surface. An incident electron current, I_P, is diffracted into a specular beam, I_R, and nonspecular beams, I'_R. The diffracted current is modulated by the angle between I_P and the surface normal, *n*, and by the spacing between the first and second layers of the solid (d_{12}), the second and third layers (d_{23}), and so on.

An accurate LEED analysis requires that several key physical processes be modeled correctly. The scattering of an electron from an atom is a fundamental feature, and, as mentioned earlier, the analysis must accurately account for the multiple scattering of electrons. Models developed in the early 1970's and based on a technique referred to as the layer-KKR (Korringa, Kohn, and Rostoker) formalism were able to model correctly the single and multiple scattering of electrons by a lattice of atoms (*5, 19*). Because the layer-KKR formalism can be computationally intensive, various perturbation techniques have been developed to treat multiple electron scattering. When applicable, such perturbation techniques

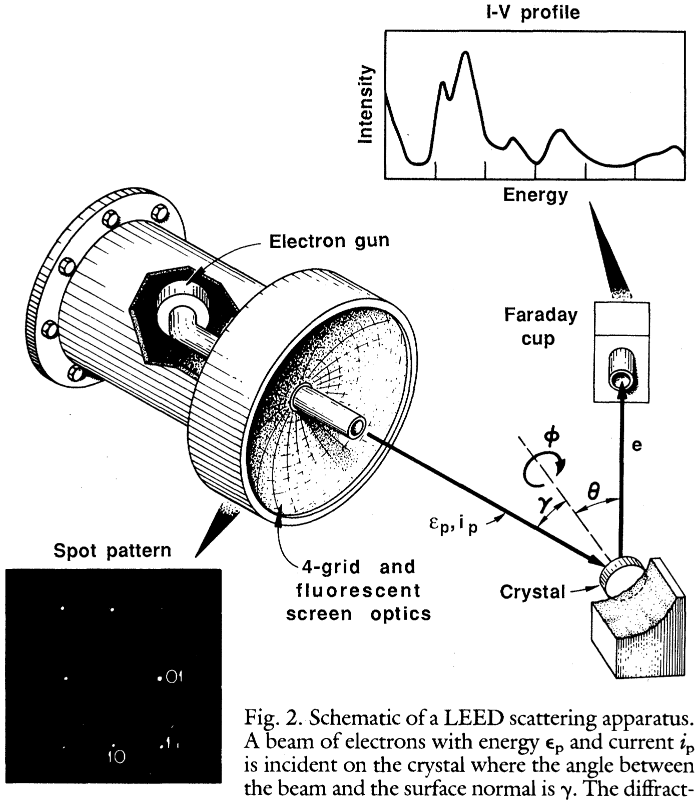

Fig. 2. Schematic of a LEED scattering apparatus. A beam of electrons with energy ϵ_p and current i_p is incident on the crystal where the angle between the beam and the surface normal is γ. The diffracted current, *e*, is measured as a function of the azimuthal angle in the surface, ϕ, and the scattering angle relative to the surface normal, θ.

can greatly reduce the amount of computer time required for a LEED analysis.

It is also essential to model correctly the refraction and attenuation of the low-energy electrons and the defocusing of the beam caused by the thermal motion of the atoms. The refraction and attenuation are simulated by the use of a complex optical potential. In analogy with optics, the electron propagation is modified by a complex potential in which the real component acts as a potential energy term and the imaginary component accounts for the attenuation of the electron beam (*5*). The electron optical potential can be energy dependent, and its parameters are usually determined by comparing calculated and measured *I-V* spectra. The attenuation due to vibrations of the surface atoms is modeled by a rigid lattice of "blurred atom" scatterers, in which the amount of blurring is determined by a Debye model for the thermal vibrations of the atoms (*19, 20*).

An important test of any LEED analysis is the sensitivity of the determined atomic structure to the choice of the scattering potential, the electronic and thermal attenuation, and so on. Tests performed to assess the effects of varying these nonstructural parameters have shown that small variations do not significantly alter the structural conclusion of a LEED analysis (*21*). In order to determine an optimal structure, however, a large number of models need to be tested.

LEED analysis is limited by both calculational and experimental aspects. To ensure that the predicted structure is converged and unique, many calculations—sometimes as many as several hundred—are performed in which both structural and nonstructural parameters are varied systematically. Therefore, the speed and size of computers have always limited the size of the surface cell that can be studied. Supercomputers have made it possible to apply LEED analysis to increasingly complex surfaces.

Advances in experimental surface analysis systems and data acquisition techniques have also contributed to the improved quality of LEED analysis. The diffracted current is measured either directly with electron detectors such as a Faraday cup, or indirectly by means of the light emission from a fluorescent display. Our LEED analyses are based on *I-V* spectra measured with a Faraday cup; photodetector systems have been described recently (*22*).

In our analyses, a crystal that has been aligned, cut, and polished to expose a selected surface is mounted on a manipulator capable of translation and rotation in vacuum. The crystal is prepared so that after cleaning it has a well-ordered crystal surface. This sample is positioned in front of the LEED analyzer, which consists of an electron gun, a set of retarding grids for energy analysis, a fluorescent screen, and a movable Faraday cup (Fig. 2). The gun produces a well-collimated beam of electrons (divergence ~1°) in the energy range 20 to 500 eV. (The beam divergence is typical for LEED guns presently used in structure analysis. Guns capable of producing smaller divergence are being developed for studies of long-range order on surfaces; these better guns may be used in the next generation of LEED spectrometers.) The electrons backscattered from the sample pass through a set of grids that transmits only electrons having energy near that of the electrons emitted from the gun (called the primary energy). The transmitted electrons are displayed on the fluorescent screen; an example of the displayed LEED beams, referred to as the LEED pattern, is shown in the lower inset of Fig. 2.

If a specific diffraction beam (a spot on the LEED pattern) is observed as the energy is changed, its current will be modulated by interference caused by scattering from deeper atomic planes. The *I-V* dependence is illustrated in the upper inset of Fig. 2; such an *I-V* spectrum would be used in a LEED structure analysis. Because the Faraday cup is simply a movable retarding field analyzer with a small aperture that permits both energy and spatial resolution of the backscattered electrons, it can track the elastically diffracted beam as the primary energy is changed. The Faraday analyzer has two advantages over most photometer systems: (i) it can be positioned anywhere in the half-space above the sample (except for a small region near the electron gun), so that the diffracted beams can be measured to almost grazing incidence ($\theta = 90°$); and (ii) the electron-optics of the cup's retarding field is more uniform than that of a grid analyzer, so that the cup can be operated with a smaller retarding potential to reduce the collection of inelastically scattered electrons.

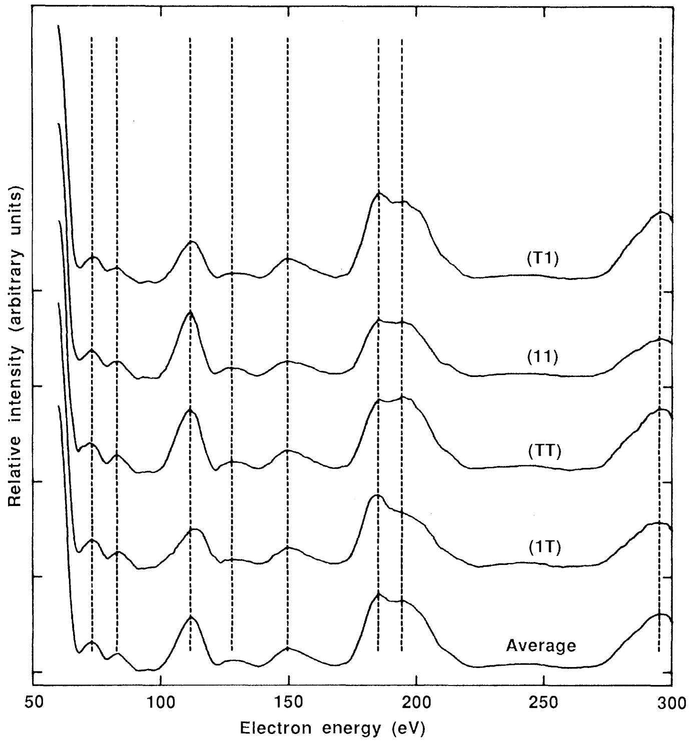

Fig. 3. Experimental *I-V* spectra for the four symmetric {11} LEED beams from a Cu(100) surface at normal incidence and the average *I-V* spectrum for the four.

Low-energy electron scattering is sensitive to imperfections. The amount of current in a particular beam can be changed by the amount of the electron gun's beam divergence, the magnetic and electric fields near the sample, the alignment of the sample with respect to the incident beam, and imperfections in the crystallinity of the surface. The errors introduced in measuring the current are not random, however. For example, any of the imperfections mentioned degrade the beam's *I-V* spectra in a systematic way. This in turn introduces systematic errors in the structure analysis. Nevertheless, a technique has been developed that reduces the influence of some of the systematic errors on the results of the final analysis.

The quality of the experimental *I-V* spectra can be enhanced by measuring *I-V* spectra for all groups of LEED beams that should be symmetrically equivalent. The group's *I-V* spectra are then averaged to produce an equivalent LEED beam spectrum for eventual analysis. For example, there are four equivalent beams in the {11} LEED beam set for a Cu(100) surface when the primary beam is at normal incidence (Fig. 3). The top four spectra of Fig. 3 were measured after the sample was aligned as nearly normal as possible to the primary beam and after adjustments were made so that the four spectra were as similar to each other as possible. (Because of imperfections in the LEED diffractometer and the surface morphology, however, discrepancies between the four $\{11\}$ I-V spectra do exist.) These spectra were averaged to yield an equivalent (11) LEED beam spectrum for analysis (Fig. 3). Other sets of nondegenerate LEED beams are measured and averaged to increase the experimental database. This equivalent beam averaging (EBA) technique improves the agreement between measured and calculated I-V spectra and therefore increases the accuracy of a LEED analysis (*22, 23*). The procedure takes advantage of the reflection coefficient, which varies slowly as a function of the incidence angle of the electrons. In other words, although individual beams in a symmetry set are sensitive to a symmetry-breaking imperfection, the total current diffracted into a given symmetrical set is not so sensitive; current lost to one beam, say the $(1\bar{1})$ beam in Fig. 3, is added to another of the set, such as the $(\bar{1}\bar{1})$ beam. The total current for a selected LEED spectrum thus more closely represents the "perfect" scattering condition. The improvements in analysis as a result of the EBA procedure can be quite remarkable; for example, sensitivity to atomic positions can be better than 0.01 Å.

Atomic Arrangements of Metal Surfaces

Multilayer relaxations of monatomic metal surfaces. The analysis of the Al(110) surface is a good example of surface multilayer relaxation. As mentioned earlier, the Al(110) surface was one of the first for which relaxation of the outermost layer was identified. The amount of relaxation was not precisely known from the early work, however, because the values ranged from 5 to 15% contraction with respect to the bulk (110) interplanar spacing of 1.43 Å. Two independent groups have reexamined the Al(110) surface using present-day LEED techniques (*24, 25*). They found that the first atomic layer was contracted toward the bulk by 8.5% with respect to the bulk spacing; more important, they showed that deeper atomic layers were also displaced from bulk lattice positions.

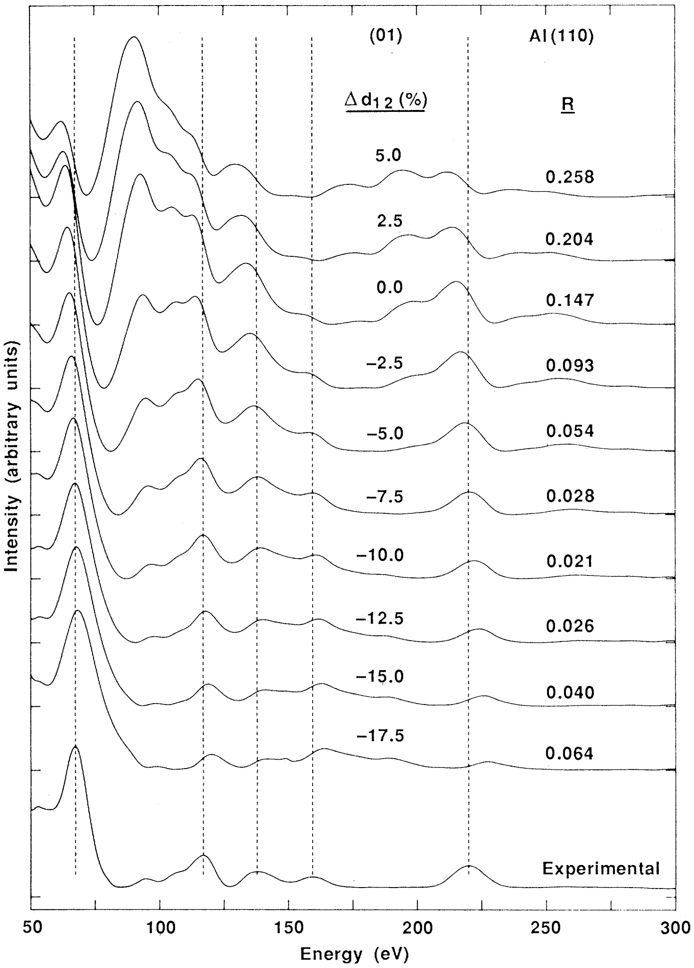

Fig. 4. Comparison of the measured (01) beam I-V spectrum for the Al(110) surface with the calculated (01) beam spectra at selected first-layer interplanar distances. For illustrative purposes, the calculated spectra were made for a second layer expansion of 5.9%.

When a surface layer is displaced away from its bulk position, diffraction peaks in an I-V spectrum shift in energy and change in relative intensity as a result of the changing interference between electrons scattered at the surface and the underlying atomic planes. Consider calculated I-V spectra for the (01) beam from Al(110) as a function of Δd_{12}, which is the amount of change in the first interlayer spacing (Fig. 4). Visual inspection of the calculated spectra for selected Δd_{12} can be used to determine the best agreement with the experimental I-V spectrum. The calculated spectra for $-7.5\% \leq \Delta d_{12} \leq -12.5\%$ clearly are in better agreement with experiment than the others in Fig. 4. The comparison can be refined by use of reliability factor (R factor) analysis, in which the agreement between two spectra is quantified by computing a sum of point-to-point functional differences and then normalizing the sum to a standard. Typically, the R factor is normalized so that 0 represents perfect agreement and 1 denotes that the two curves do not correlate. Each calculated spectrum of Fig. 4 has been compared with the experimental spectrum by means of the R factor defined by Zanazzi and Jona (*26*). The lowest R value occurs for the spectrum calculated for $\Delta d_{12} = -10\%$, which is consistent with visual inspection. R factor analysis improves the sensitivity of LEED analysis, especially when extended to consider displacements of more than one layer.

The displacements of the first and second atomic layers in Al(110) are clearly evident by examination of the R factor topograph shown in Fig. 5, in which the total R factor for eight beams is displayed as a function of changes in both the first and second interlayer spacings. The nonstructural parameters used in the Al(110) analysis were also tested to produce calculated spectra having the best agreement with the experimental spectra and to determine the sensitivity of the structural conclusions to the choice of these parameters (*24*). The final results were:

$$d_{12} = 1.310 \pm 0.014\ \text{Å}\ (\Delta d_{12} = -8.5 \pm 1.0\%)$$
$$d_{23} = 1.510 \pm 0.016\ \text{Å}\ (\Delta d_{23} = +5.5 \pm 1.1\%)$$
$$d_{34} = 1.463 \pm 0.019\ \text{Å}\ (\Delta d_{34} = +2.2 \pm 1.3\%)$$
$$d_{45} = 1.455 \pm 0.022\ \text{Å}\ (\Delta d_{45} = +1.6 \pm 1.6\%)$$
$$d_{\text{bulk}} = 1.43\ \text{Å}$$

The error limits were chosen by analyzing the predicted atomic structure for a number of calculational models in which the nonstructural parameters were varied over physically reasonable limits. This analysis tests systematic errors as well as random errors. Spectra calculated for this multilayer relaxation model of the Al(110) surface are in good agreement with the corresponding experimental spectra (Fig. 6), and the total eight-beam R factor is 0.032.

Andersen and colleagues (*25*) have also performed an extensive LEED analysis for the Al(110) surface. Their analysis yielded:

$$\Delta d_{12} = -8.6 \pm 0.8\%$$
$$\Delta d_{23} = +5.0 \pm 1.1\%$$
$$\Delta d_{34} = -1.6 \pm 1.2\%$$
$$\Delta d_{45} = +0.1 \pm 1.3\%$$

In this analysis the errors were assumed to be strictly random, and a confidence interval was determined from a statistical analysis of the data. The calculated results of this analysis were also in good agreement with experimental I-V spectra. The agreement between

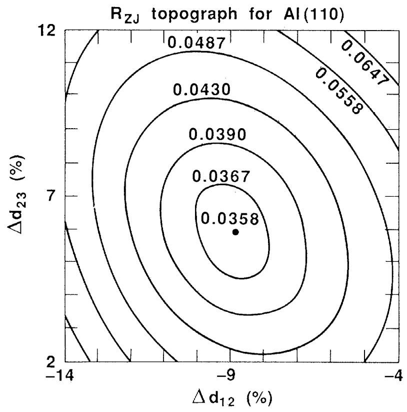

Fig. 5. *R* factor topograph for eight LEED beams from the Al(110) surface as a function of changes of the first and second interplanar spacings. R_{ZJ} factor is defined by Zanazzi and Jona (*26*).

the two independent analyses is better than 0.01 Å for the first two interlayer relaxations.

The Al(110) surface was selected as an example of how LEED analysis can be used to determine multilayer relaxation in surfaces of monatomic metals. Several groups have investigated a wide range of surfaces, all of which exhibit multilayer relaxation (*9–11, 23–25*). The outer atomic layers of low-index surfaces, such as Al(110), exhibit relaxations perpendicular to the surface. Atomic layers of high-index surfaces, however, sometimes exhibit parallel as well as perpendicular relaxations. For example, the truncated bulk W(211) surface has atomic layers stacked such that the atoms of its second layer are not centered, or symmetrically placed, with respect to the rectangular unit cell of its top layer. As shown by a LEED *I-V* analysis (*27*), the top layer of the W(211) surface has both parallel and perpendicular relaxations such that its second-layer atoms are more symmetrically placed. Therefore, even though the LEED spot pattern is (1×1), the W(211) surface is significantly distorted from the hypothetical truncated bulk surface. Other high-index surfaces have also been shown to exhibit both perpendicular and parallel relaxations (*10, 11*).

Theoretical understanding of the multilayer relaxation at metallic surfaces has progressed along with experimental studies. Finnis and Heine (*7*) demonstrated that, unless the electronic charge for the truncated bulk surface was redistributed, the repulsive ion-ion interaction would cause the first interlayer spacing to be expanded from the bulk value. If the electronic charge was redistributed as if electrons had surface tension, however, then the first interlayer spacing of any metallic surface would be contracted.

Subsequent theoretical work has improved the model, making possible more quantitative predictions. Landman and colleagues (*8*) have argued that any redistribution of electronic charge would not be completely accommodated within only one interlayer spacing, and, although interlayer spacings must eventually approach the bulk value, the surface charge redistribution would alter deeper interlayer distances. With the use of various standard models for surface charge distributions, it was demonstrated that a damped, oscillatory relaxation of atomic layers should occur; that is, the surface layer should contract toward the second, the second expand with respect to the third but by a smaller amount, the third contract by an even smaller amount, and so on. In this work, however, no attempt was made to allow the assumed electronic densities to respond self-consistently to the calculated relaxations, which were predicted to be quite large and deep.

Several theoretical studies have improved quantitatively on Landman's work by allowing for better self-consistency, including screening, and by performing total-energy calculations (*28–30*). The most accurate theoretical predictions are in reasonable agreement with the relaxations obtained in the LEED analyses. In addition, one theoretical study used a simple model for considering some high-index surfaces (*31*). The theoretical results show that layer relaxations can have components both perpendicular and parallel to the surfaces, as was also found in several LEED experiments (*10, 11, 27*).

The Al(110) surface was used to illustrate the type of multilayer relaxation results that can be obtained by LEED analysis. Results from the most complete theoretical treatment of this surface are therefore of interest. Ho and Bohnen (*29*) performed first-principle, self-consistent, total-energy, electronic structure calculations for aluminum slabs composed of up to 15 atomic layers. Their results for the multilayer relaxation of Al(110) were:

$$\begin{aligned}\Delta d_{12} &= -6.8 \pm 0.5\% \\ \Delta d_{23} &= +3.5 \pm 0.5\% \\ \Delta d_{34} &= -2.0 \pm 0.5\% \\ \Delta d_{45} &= +1.6 \pm 0.5\%\end{aligned}$$

The error limits were calculated from total energy differences derived for selected convergence tests. These results are all within about 0.025 Å of the values obtained by LEED analyses (*24, 25*) and by a previous theoretical model (*28*).

Metallic alloy surfaces. The techniques and theories for surface relaxations are also being applied to more complex systems, such as binary metal alloys, and the results have been both reassuring and surprising. LEED analyses of several alloy surfaces have identified their atomic arrangements. Even though the number of alloy surfaces analyzed is small, the complexity of the surface-induced changes in their atomic structure is apparent.

The NiAl(110) surface will serve to illustrate the quality of LEED analysis that is possible for an alloy surface and how surface forces affect a binary system (*16*). NiAl is an intermetallic compound that orders in a CsCl structure, that is, it has two interpenetrating simple cubic sublattices of nickel and aluminum, forming a body-centered cubic lattice. Therefore, its bulk (110) planes consist of alternating rows of nickel and aluminum atoms along the [001] direction (Fig.

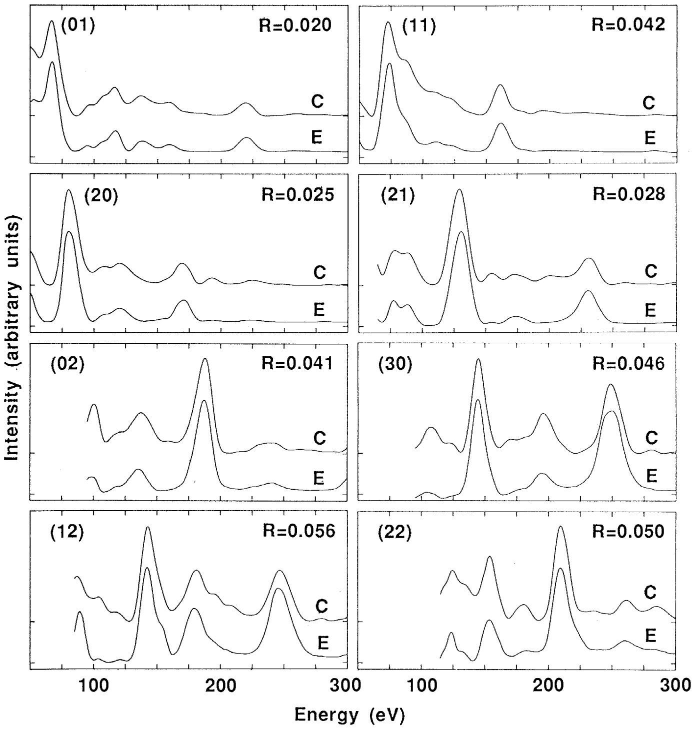

Fig. 6. Calculated (C) and experimental (E) *I-V* spectra for eight LEED beams for Al(110).

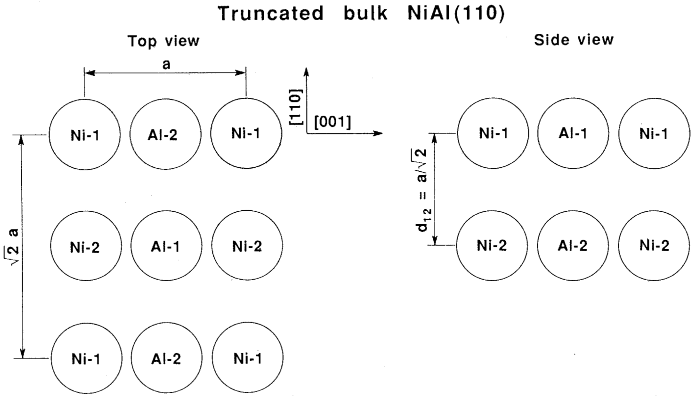

Fig. 7. Ball model of the truncated bulk NiAl(110) surface; Al refers to aluminum atoms in the unit cell, Ni refers to nickel atoms, −1 refers to surface layer atoms, −2 refers to second layer atoms, and *a* is the bulk unit cell length (~2.88 Å). LEED analysis indicates that this model is incorrect.

7). A NiAl(110) surface can be prepared so that it (i) is clean (that is, so that only nickel and aluminum are detected by techniques such as Auger electron spectroscopy that measure atomic concentrations at a surface); (ii) is well ordered, as demonstrated by a well-focused LEED pattern with low background intensity; and (iii) has approximately the same stoichiometry as the bulk, as determined by quantitative Auger analysis studies and by an x-ray photoemission study (*32*). The LEED pattern is (1×1) with respect to the bulk crystal; that is, parallel to the surface, the unit cell has the same dimensions as the bulk unit cell.

The NiAl(110) surface was analyzed by measuring EBA *I-V* spectra for 14 nondegenerate LEED beams, which were then compared to *I-V* spectra calculated for selected structural models. These comparisons identified a novel feature of the NiAl(110) surface: a surface reconstruction in which nickel rows are contracted toward the bulk and aluminum rows are expanded away from the bulk. This model produced the best agreement between calculated and experimental spectra. For example, the calculated *I-V* spectrum for the rippled surface model has better agreement with the experimental (10) spectra than spectra calculated for either a truncated bulk surface or a model in which the surface layer is forced to remain coplanar but is relaxed to maximize the agreement to the data (Fig. 8). Deeper relaxations were also considered in the LEED analysis, and the best structure is one in which both the first and second layers are rippled. The displacements are:

$$\Delta d_{12}^{\mathrm{Ni}} = -4.6\%$$
$$\Delta d_{12}^{\mathrm{Al}} = +5.2\%$$
$$\Delta d_{23}^{\mathrm{Ni}} = +1\%$$
$$\Delta d_{23}^{\mathrm{Al}} = +2\%$$

The truncated bulk ball model of NiAl(110) has been modified to show the effects that the surface induced on the nickel and aluminum atoms (Fig. 9). The 14-beam *R* factor for this surface is 0.053, which is comparable in quality to that of better analyses of monatomic metal surfaces. The rippled reconstruction of Fig. 9 has been corroborated by a medium-energy ion-scattering experiment (*33*).

Several other experiments have shown that the atomic arrangements of alloy surfaces can be unusual. For example, a low-energy ion-scattering experiment on $Cu_3Au(100)$ and a LEED analysis of the $Ni_3Al(100)$ alloy indicated that each of the surfaces terminates in a unique way (*14, 15*). The Cu_3Au and the Ni_3Al crystals have the same $L1_2$ crystal structure; therefore, the (100) stacking sequence is such that a layer of type A atoms alternates with a 50-50 mixed layer of type A and B atoms. The surface could thus terminate in either or both types of layers (because of step imperfections). These experiments have indicated that only the mixed layer is at the surface. Another example of a surface effect is the ordering of an aluminum overlayer on the (111) surface of a Cu–16%Al alloy (*12*). The aluminum atoms are randomly distributed in the bulk; however, annealing the crystal to approximately 570 K not only segregates aluminum atoms to the surface but also causes them to form an ordered net on the (111) surface. The LEED analysis also indicated that the aluminum atoms are placed in face-centered cubic stacking positions. Finally, Gauthier and co-workers (*13*) found that the surface stoichiometry of an alloy can be altered in a complex fashion. For example, $Pt_{78}Ni_{22}$ is a substitutionally random alloy; that is, the alloy is crystalline but the probability of a platinum or nickel atom occupying a specific lattice has a random distribution. At the surface, however, the first layer was platinum enriched to a concentration of about 99%, the second layer was depleted to about 30%, and the third layer was enriched by a small amount.

Future Research

Interpreting research results obtained in areas such as photoemission and catalysis requires that the atomic arrangement of the surface be understood. There are several examples of alloys in which the photoemission spectra and calculated photoelectron yields do not agree. The disagreement could be because the electronic structure potentials in the surface region are not correct. However, the calculations were performed for truncated bulk atomic arrangements. If surface relaxations were available for the alloy surfaces, more accurate potentials could be calculated and improved electronic structures might result. Cluster calculations for chemical reactions at surfaces also are performed with truncated bulk atomic arrangements. The relaxations for a surface involved in a chemical reaction must be known because some reactions are sensitive to small changes in atomic coordination or bond lengths (or both). The problem of surface relaxations in the presence of an adsorbate is even more complex because the adsorbate atom causes a different electronic distribution from that for a clean surface.

Fig. 8. Comparison of calculated *I-V* spectra for the (10) beam from NiAl(110) for the truncated bulk (TB), the relaxed coplanar surface (CP), and the rippled surface (R) with the measured spectrum (E).

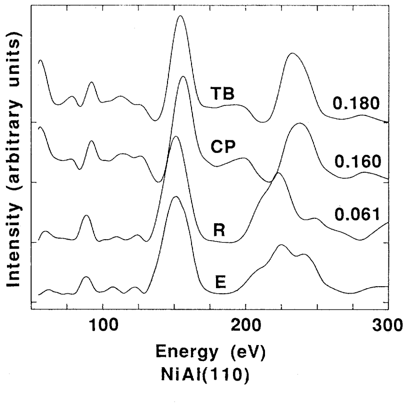

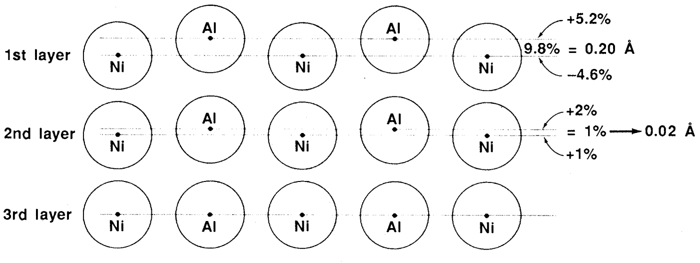

Fig. 9. Ball model of the rippled NiAl(110) surface: side view.

Conclusions

The examples discussed in this article illustrate how the current theoretical and experimental research on surfaces has led to a better understanding of the microscopic origins and energetics of surface cohesion. It has been shown that electrostatic forces induced by the creation of a surface alter the atomic arrangements at the surface. In some cases, especially directionally bonded solids such as semiconductors, the surface is reconstructed into a crystallographic group that is different from the bulk. However, all surfaces, even those with the same two-dimensional symmetry as the bulk, are altered from the hypothetical truncated bulk. The induced forces are strong enough to create a multilayer relaxation of the outermost atomic planes.

Research on surface crystallography has been extended to surfaces of binary metal alloys. The atomic displacements induced by the surface forces are complex, but, as demonstrated by the successful analysis of the reconstruction of the NiAl(110) surface, many problems are tractable and will provide important additional information concerning the atomic interactions in nonuniform environments.

REFERENCES AND NOTES

1. J. A. Golovchenko, *Science* **232**, 48 (1986).
2. K. Takayanagi, Y. Tanishiro, S. Takahashi, M. Takahashi, *Surf. Sci.* **164**, 367 (1985).
3. R. M. Tromp, R. J. Hamers, J. E. Demuth, *Science* **234**, 304 (1986).
4. P. J. Estrup, *Chem. Phys.* **35**, 205 (1984).
5. G. E. Laramore and C. B. Duke, *Phys. Rev. B* **5**, 267 (1972).
6. D. W. Jepsen, P. M. Marcus, F. Jona, *ibid.* **6**, 3684 (1972).
7. M. W. Finnis and V. Heine, *J. Phys. F* **4**, L37 (1974).
8. U. Landman, R. N. Hill, M. Mostoller, *Phys. Rev. B* **21**, 448 (1980).
9. H. L. Davis and J. R. Noonan, *Surf. Sci.* **126**, 245 (1983).
10. D. L. Adams and C. S. Sorensen, *ibid.* **166**, 495 (1986).
11. J. Sokolov, F. Jona, P. M. Marcus, *Solid State Commun.* **49**, 307 (1984).
12. R. J. Baird, D. F. Ogletree, M. A. van Hove, G. A. Somorjai, *Surf. Sci.* **165**, 345 (1986).
13. Y. Gauthier, Y. Joly, R. Baudoing, J. Rundgren, *Phys. Rev. B* **31**, 6216 (1985).
14. D. Sondericker, F. Jona, P. M. Marcus, *ibid.* **33**, 900 (1986).
15. T. M. Buck, G. W. Wheatley, L. Marchut, *Phys. Rev. Lett.* **51**, 43 (1983).
16. H. L. Davis and J. R. Noonan, *ibid.* **54**, 566 (1985).
17. C. J. Davisson and L. H. Germer, *Phys. Rev.* **30**, 705 (1927).
18. R. L. Park and H. E. Farnsworth, *Surf. Sci.* **2**, 527 (1964).
19. D. W. Jepsen, P. M. Marcus, F. Jona, *Phys. Rev. B* **5**, 3933 (1972).
20. C. B. Duke and G. E. Laramore, *ibid.* **2**, 4765 (1970); G. E. Laramore and C. B. Duke, *ibid.* p. 4783.
21. H. L. Davis and J. R. Noonan, in *Determination of Surface Structure by LEED*, P. M. Marcus and F. Jona, Eds. (Plenum, New York, 1984), p. 215.
22. K. Heinz and K. Muller, in *Structural Studies of Surfaces*, G. Hohler, Ed. (Springer, Berlin, 1982).
23. J. R. Noonan and H. L. Davis, *J. Vac. Sci. Technol.* **17**, 194 (1980); H. L. Davis and J. R. Noonan, *Phys. Scr.* **T4**, 141 (1983).
24. J. R. Noonan and H. L. Davis, *Phys. Rev. B* **29**, 4349 (1984).
25. J. N. Andersen, H. B. Nielsen, L. Petersen, D. L. Adams, *J. Phys. C* **17**, 173 (1984).
26. E. Zanazzi and F. Jona, *Surf. Sci.* **62**, 61 (1977).
27. H. L. Davis and G.-C. Wang, *Bull. Am. Phys. Soc.* **29**, 221 (1984).
28. R. N. Barnett, U. Landman, C. L. Cleveland, *Phys. Rev. B* **28**, 1685 (1983).
29. K. M. Ho and K. P. Bohnen, *ibid.* **32**, 3446 (1985).
30. C. L. Fu, S. Ohnishi, E. Wimmer, A. J. Freeman, *Phys. Rev. Lett.* **53**, 675 (1984).
31. R. N. Barnett, U. Landman, C. L. Cleveland, *ibid.* **51**, 1359 (1983).
32. R. Gaylord, private communication.
33. S. M. Yalisove and W. R. Graham, *Bull. Am. Phys. Soc.* **31**, 325 (1986).

34. Sponsored by the Department of Energy, Division of Materials Sciences, under contract DE-AC05-840R21400 with Martin Marietta Energy Systems, Inc.

Electron- and Photon-Stimulated Desorption: Probes of Structure and Bonding at Surfaces

THEODORE E. MADEY

Techniques for analyzing the structure and composition of solid surfaces with electron and photon beams often cause radiation damage in samples. Damage-producing processes compete with information-producing events during measurements, and beam damage can be a serious perturbation in quantitative surface analysis. There are, however, substantial benefits of electron- and photon-stimulated damage processes for studying molecules adsorbed on surfaces. Direct information about the geometric structure of surface molecules can be obtained from measurements of the angular distributions of ions released by electron- or photon-stimulated desorption. The directions of ion emission are determined by the orientation of the surface bonds that are ruptured by beam irradiation. Moreover, photon-stimulated desorption studies that make use of synchrotron radiation reveal the fundamental electronic excitations that lead to bond-breaking processes at surfaces. These measurements provide new insights into radiation-damage processes in areas as diverse as x-ray optics and semiconductor electronics.

ELECTRONS AND PHOTONS ARE WIDELY USED AS PROBES for surface chemical and structural analysis in a number of surface measurements, including Auger electron spectroscopy, x-ray photoelectron spectroscopy, and scanning electron microscopy. The assumption in most of these studies is that the bombarding electrons and photons are relatively unperturbing probes that do little damage to the structure or composition of the surface being characterized. In fact, electron and photon bombardment can induce various bond-breaking processes at surfaces that are analogous to gas-phase electron- and photon-induced dissociation. In most surface analyses, this radiation-induced rupture of surface bonds is a nuisance to be avoided or minimized; in the cases described here, analysis of the surface dissociation (desorption) products can be beneficial by providing insights into the structure and bonding of surface species. This information comes from electron-stimulated desorption (ESD) and photon-stimulated desorption (PSD) studies of surfaces, which are the subject of much experimental and theoretical interest (*1–5*).

In ESD and PSD, beams of energetic electrons or photons (typically about 10 to more than 1000 eV) incident on surfaces

---

The author is an NBS fellow in the Surface Science Division at the National Bureau of Standards, Gaithersburg, MD 20899.